DONNAY, J. D. H. (1977). *Acta Cryst.* A33, 979–984.
DONNAY, J. D. H. & LE PAGE, Y. (1978). *Acta Cryst.* A34, 584–594.
EDENHARTER, A., NOWACKI, W. & WEIBEL, M. (1977). *Schweiz. Mineral. Petrogr. Mitt.* 57, 1–16.
FISCHER, W. & KOCH, E. (1983). *Acta Cryst.* A39, 907–915.
GABE, E. J. (1970). *Crystallographic Computing*, edited by F. R. AHMED, pp. 331–335. Munksgaard. Copenhagen.
KENNARD, O., SPEAKMAN, J. C. & DONNAY, J. D. H. (1967). *Acta Cryst.* 22, 445–449.
LE PAGE, Y. & GABE, E. J. (1979). *J. Appl. Cryst.* 12, 464–466.
PARTHÉ, E. & GELATO, L. (1984). *Acta Cryst.* A40, 169–183.

Acta Cryst. (1984). A40, 684–688

Experimental Procedures for the Determination of Invariant Phases of Centrosymmetric Crystals

BY BENJAMIN POST*

Polytechnic Institute of New York, Brooklyn, New York, USA

AND JOSEPH NICOLOSI† AND JOSHUA LADELL

Philips Laboratories, Briarcliff Manor, New York, USA

(*Received* 28 *April* 1984; *accepted* 11 *June* 1984)

Abstract

The [222] *n*-beam pattern of germanium has been recorded using Cu $K\alpha_1$ radiation and newly developed instrumentation. The asymmetric unit of the pattern contains 17 interaction maxima. At least one invariant triplet phase may be derived from each maximum. Two of the latter are considered unsuitable for phase determination owing to overlap with adjacent peaks. The phases of the remaining 15 were determined. Relevant experimental data are presented and from these the validity of the authors' phase assignments can be readily checked. Techniques for indexing *n*-beam patterns and for improving the visibility of triplet phase interactions are discussed. It is shown that procedures for improving the visibility of *n-beam interactions* do not necessarily lead to increased visibility of *phase indications.*

1. Introduction

One of the authors (J. Ladell) has recently completed construction of a novel four-circle single-crystal diffractometer for use in diffraction experiments. The (biaxial) diffractometer utilizes inclination geometry, features two mutually orthogonal crystal rotation axes, and provides for moving the detector on a spherical surface. It is used in conjunction with a highly collimated and monochromatic incident beam, and provides the capability of controlling specimen orientation and detector placement with high precision. It has been used for the experimental determination of the invariant phases of perfect crystals of germanium and mosaic crystals of lead molybdate, zinc tungstate and other specimens.

In this paper we will discuss the use of this new equipment for the experimental determination of the phases of germanium. We will also discuss general aspects of *n*-beam diffraction, which, to the best of our knowledge, have not been dealt with previously.

The selection of germanium for this investigation requires some explanation. Its crystal structure is simple; all atomic positions are fixed by symmetry. The phases of all but a few very weak reflections can be easily calculated. It is, however, largely because of that simplicity that we have chosen to demonstrate the phase procedure by applying it to germanium. Relevant experimental data are given so that the reader can readily check the validity of our phase assignments by calculating the phases independently, and comparing the results with the experimental evidence and with the authors' phase assignments.

2. Experimental

Techniques for generating *n*-beam diffraction systematically and for calculating the azimuthal angles at which *n*-beam interactions occur have been discussed by Cole, Chambers & Dunn (1962) and Post (1975). Additional details, with emphasis on the application of *n*-beam diffraction to experimental phase determination, are given by Gong & Post (1983) and Post (1983).

* This author's work was supported by the National Science Foundation and in part by the Joint Services Electronics Program of the US Defense Department.

† Taken in part from the dissertation submitted to the faculty of the Polytechnic Institute of New York in partial fulfilment of the requirements for the degree Doctor of Philosophy (Physics, 1982). Present address: Philips Electronics Instruments, Mahwah, New Jersey, USA.

0108-7673/84/060684-05$01.50

The biaxial diffractometer used in this investigation utilizes a skewed arrangement of two silicon crystals to provide a *monochromatic and collimated* incident beam with a divergence of 30 to 40″ in the beam cross section. The two crystals are arranged so that the plane of diffraction involving the first crystal is rotated 45° from the plane of diffraction of the second. The crystals are in the dispersive arrangement with the angle between their diffraction vectors less than 90°. They are arranged in space so that the beam from the X-ray tube and the one diffracted from the second crystal lie in the horizontal plane (Fig. 1).

Two stepper motors control the orientation of the specimen. One rotates the entire specimen rotation assembly about the vertical axis (μ drive); the other rotates the crystal about a diffraction vector that is coincident with the horizontal axis along which the crystal is mounted (ω drive). Both rotations are monitored by computer-readable absolute-angle optical encoders, which have a resolution of $360/2^{18}$ (*i.e.* about 5″).

The settings of the counter detector are also independently controlled by two stepper motors. These can move the detector to settings above and below the horizontal plane passing through the instrument center. The latter is at the intersection of the mutually orthogonal crystal drive axes (in the polar plane). All four motors as well as other variables used in diffraction experiments (*e.g.* step sizes, dwell times *etc.*) are computer controlled. Steps as small as 0·001° can be implemented. A schematic diagram of the biaxial diffractometer is shown in Fig. 2.

The diffraction experiments were carried out using a modified version of the Renninger (1937) procedure. In addition, the detector was moved, as needed, to settings at which diffraction due to secondary (transit) reciprocal-lattice points (r.l.p.s) traversing the surface of the Ewald sphere could be directly monitored. This made possible virtually unambiguous verification of the indices assigned to those r.l.p.s (see below, § 4.2).

Two apparently equivalent settings of the crystal rotation axis relative to the incident-beam direction are shown in Fig. 3. In setting *A* the three crystal reflecting planes involved in the experiment (the two monochrocollimator crystal planes and the primary reflection of the specimen crystal) are generally in dispersive positions, *i.e.* pseudo antiparallel. In the *B* setting the monochrocollimator crystal planes arrangement is dispersive, as in setting *A*, but the primary reflection plane of the specimen crystal is in a (partially) non-dispersive arrangement. In practice, the results obtained from settings *A* and *B* differ significantly. The line profiles in setting *A* are generally broader and *n*-beam peak heights are significantly lower than in setting *B*. These will be discussed in greater detail elsewhere (Ladell, 1984).

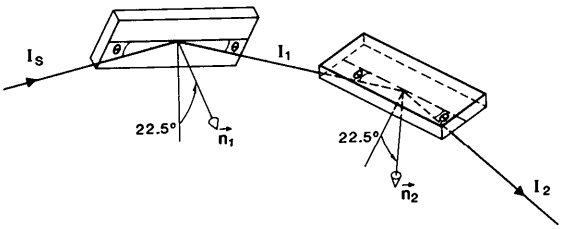

Fig. 1. Double-crystal monochrocollimator. I_s is the beam incident on the first crystal whose diffraction vector $\mathbf{n}_1$ is tilted 22·5° above the horizontal plane. I_1 is diffracted from the first and incident upon the second crystal whose diffraction vector, $\mathbf{n}_2$, is tilted 22·5° below the horizontal plane. I_2 is the collimated monochromatic beam incident on the crystal studied.

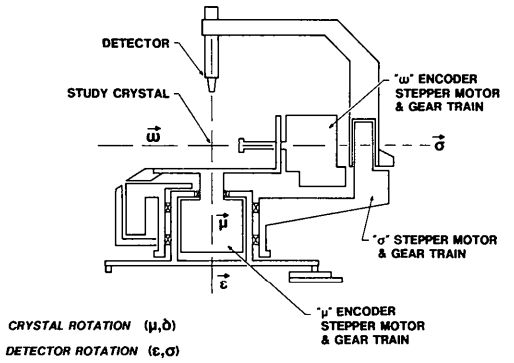

Fig. 2. Schematic diagram of the biaxial diffractometer. Crystal is rotatable about the ω axis, which is, in turn, rotatable about the vertical μ axis. Detector is independently rotatable about the σ axis, which in turn is rotatable about the μ axis.

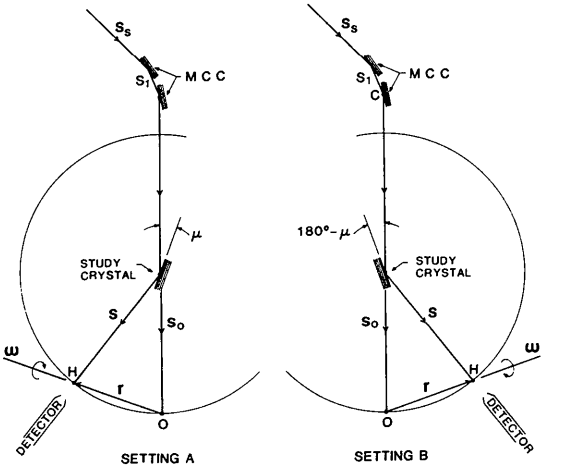

Fig. 3. Two settings of the crystal rotation axis relative to the incident-beam direction. $\mathbf{S}_s$ is the beam from the target source. $\mathbf{S}_1$ is diffracted from the first of the two monochrocollimator (MCC) crystals. $\mathbf{S}_0$ is the second diffracted beam, which is incident on the crystal studied shown for each setting at the center of the Ewald sphere. In both settings *A* and *B*, **r**, the diffraction vector of the primary reflection **H**, is collinear with **ω**, the horizontal axis of crystal rotation. **S** is the scattering vector, which defines the direction along which diffraction from the primary reflection *H* is detected. Setting *B* is obtained from setting *A* by rotating the crystal and detector (independently) about a vertical axis (normal to the page).

In the experimental procedures described below, rotations about the horizontal crystal axis (ω scans) were performed according to the right-hand rule. All transit r.l.p.s which intersect the Ewald sphere *above* the polar plane (*i.e.* the plane containing the incident beam and the ω axis, Fig. 3) are entering the sphere in setting *A*, and are emerging in setting *B*.

Setting *B* provides from two to four times as much diffracted *n*-beam intensity as *A*. In *B* patterns, the full widths at half maximum of peaks are from 1·5 to 5 times as great as the widths of maxima due to the same or symmetry-related r.l.p.s intersecting the Ewald sphere below the polar plane. In the *A* patterns, the shapes and peak intensities of such pairs of maxima due to r.l.p.s which intersect the Ewald sphere above and below the polar plane are essentially identical. Maxima in *A* were better resolved than equivalent maxima in the *B* arrangement; *A* was therefore used for the experiments described below.

The original intensity data were recorded in steps of 0·005°, with fixed dwell times of 4 s per step. They were stored in the computer on disk files, and could be retrieved for plotting, using appropriate scales which emphasized the quantities of interest.

3. Experimental results

n-beam diffraction patterns of centrosymmetric crystals display characteristic intensity enhancement on one side of each interaction maximum and intensity attenuation on the other. The sequence in which these appear is determined by the invariant phase of the group of reflections involved in the interaction. The sequence which characterizes the entry of a r.l.p. into the Ewald sphere is reversed when the same r.l.p. emerges from the sphere (Post, 1979).

210 r.l.p.s enter and leave the Cu $K\alpha_1$ Ewald sphere in a 360° rotation of germanium about [222]. Only 204 of the 420 possible interactions yield appreciable *n*-beam intensities. The remaining 216 all involve the very weak primary reflection 222 in addition to one strong reflection ($h+k+l=4n$) and one 'forbidden' reflection ($h+k+l=4n+2$) (*i.e.* the transit and coupling reflections). Combinations of two very weak or absent reflections and one strong reflection generate *n*-beam interactions with negligible intensities (James, 1963). They are of no importance in our phase-determination procedure. The indices of the 102 r.l.p.s, which generate the 'strong' reflections, as well as those of their coupling terms are therefore all of odd parity.

Table 1. *n-beam interaction maxima*

	h k l transit	*h k l* coupled	φ	2β	Intensity asymmetry†	Dir‡	Phase
1	$\bar{5}\,1\,3$	$7\,1\,\bar{1}$	0·11	28·02	efa	*L*	+
2	$\bar{3}\,\bar{1}\,3$	$5\,3\,\bar{1}$	0·48	82·74	efa	*L*	+
3	$\bar{1}\,\bar{1}\,1$	$3\,3\,1$	1·79	123·57	efa	*L*	+
4	$\bar{1}\,\bar{1}\,3$	$3\,3\,\bar{1}$	4·82	129·64	afe	*L*	−
5	$\bar{3}\,1\,5$	$5\,1\,\bar{3}$	7·67	75·34	efa	*L*	+
6	$1\,5\,1$	$1\,\bar{3}\,1$	7·92	104·16	ovlp	*E*	?
7	$1\,5\,3$	$1\,\bar{3}\,\bar{1}$	8·125*	43·75	efa	*E*	−
8	$\bar{1}\,5\,\bar{1}$	$3\,\bar{3}\,3$	11·44	97·12	afe	*E*	+
9	$\bar{1}\,1\,5$	$3\,1\,\bar{3}$	11·70	105·18	afe	*L*	−
10	$\bar{5}\,3\,3$	$7\,\bar{1}\,\bar{1}$	14·27	28·55	afe	*L*	−
11	$1\,3\,\bar{1}$	$1\,\bar{1}\,3$	15·84	148·32	afe	*E*	+
12	$\bar{3}\,5\,\bar{1}$	$5\,\bar{3}\,3$	16·03	60·15	ovlp	*E*	?
13	$\bar{3}\,3\,5$	$5\,\bar{1}\,\bar{3}$	16·18	60·15	afe	*L*	−
14	$\bar{1}\,3\,5$	$3\,\bar{1}\,\bar{3}$	22·26	82·74	efa	*L*	+
15	$1\,1\,3$	$1\,1\,\bar{1}$	24·58	169·15	afe	*L*	−
16	$1\,5\,\bar{1}$	$1\,\bar{3}\,3$	26·52	105·18	efa	*E*	−
17	$\bar{5}\,3\,1$	$7\,\bar{1}\,1$	27·91	28·02	efa	*L*	+

* four-beam interaction.

† afe means attenuation followed by enhancement; efa means enhancement followed by attenuation; ovlp means overlapping interactions.

‡ *E* means upon entering the Ewald sphere; *L* means upon leaving the Ewald sphere.

The [222] pattern may be divided into twelve symmetry-related 30° regions, each containing 17 maxima. These represent the asymmetric units of the pattern. Each unit is repeated by reflection across boundaries at 0, 30, 60° *etc.* The number of r.l.p.s entering the Ewald sphere in any 30° region may differ from the number leaving. The same number of r.l.p.s enter and leave the Ewald sphere in a 60° region.

A 40° portion of the [222] *n*-beam pattern of germanium is shown in Fig. 4. Approximately 5° have been added, on both sides of the asymmetric 30° region, to illustrate the reflection of maxima across boundaries at 0 and 30°. The seventeen maxima in the 0–30° region are listed in Table 1. The indices of the transit r.l.p.s and their coupling terms are given

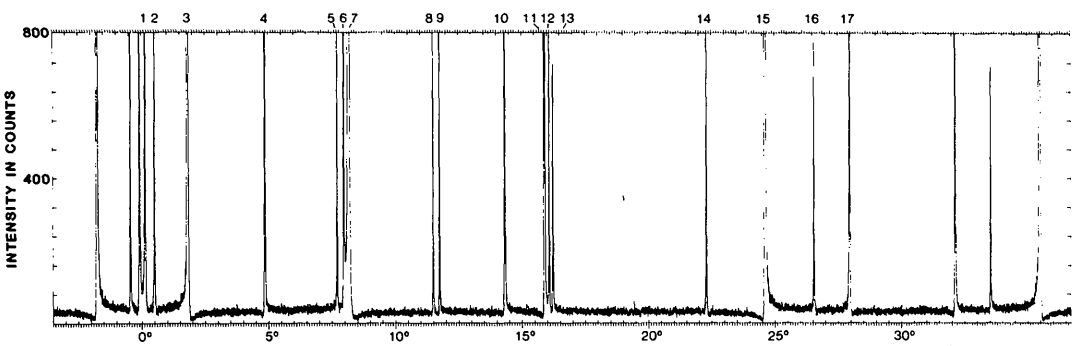

Fig. 4. The [222] *n*-beam chart of germanium obtained with Cu $K\alpha_1$ radiation.

in columns 1 and 2. The azimuthal angles (φ) at which n-beam interactions occur, and the angular intervals between entrance into and emergence from the Ewald sphere, are listed in columns 3 and 4. In the next three columns we indicate the intensity asymmetry, the direction of transit of the r.l.p. and the experimentally determined phases.

Two of the seventeen interactions (numbers 6 and 12 in Fig. 4) overlap adjacent peaks. The phases of all the remaining 15 were determined.

4. Discussion

4.1. *Visibility of n-beam interactions*

The visibility of an interaction in an n-beam pattern must be distinguished from the visibility of the phase indication given by that interaction. The former is a necessary but not sufficient condition for observation of the latter.

In n-beam patterns, the incident-beam divergence serves as a bandpass which governs the azimuthal range of the primary reflection 'seen' by the detector. The visibility of an n-beam interaction is determined by the influence of its diffracted intensity on the otherwise constant primary diffracted intensity recorded by the detector. (It is assumed that the incident-beam divergence is substantially larger than the angular width of any n-beam interaction. That is generally true.) The visibility of an interaction, therefore, approaches its maximum value as the primary reflection intensity goes to zero.

It has been pointed out (Post, 1979) that phase information, normally present in a three-beam interaction, vanishes when any one of the triplet of structure factors has zero magnitude. Those calculations, as well as the principle of continuity, indicate that very weak primary reflections generate correspondingly weak phase indications.

Consider the [222] n-beam pattern of germanium. In our experiments, with the rotating-anode generator operating at 5 kW, the recorded two-beam intensity of the 222 was 30 counts. In practice, the strength of a phase indication is usually a function of the magnitude of the intensity 'dip' observed adjacent to an interaction. The largest negative deviation from the average 222 intensity was only 22 counts. That may be compared with the intensity of the adjacent peak, which is greater than 13 000 counts. The magnitudes of dips relative to the associated maxima were usually larger in patterns using primary reflections of average intensity (Gong & Post, 1983).

4.2. *Indexing n-beam patterns*

The density of interactions in most n-beam patterns is usually very high. It may be visualized in terms of X-ray rotation photographs in which reflections, which are usually distributed among many 'layer' lines are compressed onto a single layer line. The number of possible interactions in a 360° n-beam scan is approximately equal to the number of times the surface of the Ewald sphere is crossed by r.l.p.s. Many interactions are too weak to be detected. The density of interactions, nevertheless, remains high and overlap of peaks is common.

Table 2. *Variation of n-beam interaction angles with wavelength*

	$h\,k\,l$ transit r.l.p.	$h\,k\,l$ coupling term	E/L†	φ(°) Cu $K\alpha_1$	φ(°) Cu $K\alpha_2$	$\Delta\varphi$
1	$\bar{5}\,1\,3$	$7\,1\,\bar{1}$	L	0·110	−0·634	0·724
2	$\bar{3}\,\bar{1}\,3$	$5\,3\,\bar{1}$	L	0·477	0·271	0·206
3	$1\,\bar{1}\,\bar{1}$	$3\,3\,1$	L	1·787	1·690	0·097
4	$\bar{1}\,\bar{1}\,3$	$3\,3\,\bar{1}$	L	4·819	4·724	0·095
5	$\bar{3}\,1\,5$	$5\,1\,\bar{3}$	L	7·672	7·437	0·235
6	$1\,5\,1$	$1\,\bar{3}\,1$	E	7·921	8·062	−0·141
7	$1\,5\,3$	$1\,\bar{3}\,\bar{1}$	E	8·125*	8·580	−0·455
8	$\bar{1}\,5\,\bar{1}$	$3\,\bar{3}\,3$	E	11·441	11·557	−0·116
9	$1\,\bar{1}\,5$	$3\,1\,\bar{3}$	L	11·697	11·601	0·096
10	$\bar{5}\,3\,3$	$7\,\bar{1}\,\bar{1}$	L	14·274	13·544	0·730
11	$1\,3\,\bar{1}$	$1\,\bar{1}\,3$	E	15·839	15·891	−0·052
12	$\bar{3}\,5\,\bar{1}$	$5\,\bar{3}\,3$	E	16·027	16·341	−0·314
13	$\bar{3}\,3\,5$	$5\,\bar{1}\,\bar{3}$	L	16·177	15·863	0·314
14	$\bar{1}\,3\,5$	$3\,\bar{1}\,\bar{3}$	L	22·264	22·058	0·206
15	$1\,1\,3$	$1\,1\,\bar{1}$	L	24·575	24·557	0·018
16	$1\,5\,\bar{1}$	$1\,\bar{3}\,3$	E	26·517	26·655	−0·138
17	$\bar{5}\,3\,1$	$7\,\bar{1}\,1$	L	27·905	27·162	0·743

* A four-beam interaction.

† E means upon entering the Ewald sphere; L means upon leaving the Ewald sphere.

The prior determination of accurate lattice constants and the orientation of the reciprocal unit cell with respect to the instrument axes are obvious first steps in the indexing process. These make possible the calculation of correspondingly accurate interaction angles. Ambiguities, owing mainly to overlap of maxima, will persist. These difficulties are reduced if indices are assigned simultaneously to both members of pairs of symmetry-related peaks that are mirror images of one another, and that are located at the calculated angles at which the r.l.p.s enter and leave the Ewald sphere.

Additional difficulties arise if the diffracted primary beam is not strictly monochromatic. In Table 2 we show the calculated interaction angles of the [222] n-beam pattern of germanium for Cu $K\alpha_1$ and $K\alpha_2$. Clearly, the use of $K\alpha$ radiation in n-beam patterns for phase determination will lead to indexing ambiguities and errors or uncertainties in phase assignments. The use of unfiltered incident radiation from small sources in combination with long source-to-specimen paths may yield satisfactory results in selected cases. In general, it limits the choice of primary reflections to those which diffract at relatively large Bragg angles for which the α doublet is resolvable.

With our experimental procedure it is a very simple matter to verify the assigned indices of the interactions by setting the detector to record the radiation

diffracted to the secondary r.l.p. (the 'transit' reflection). Extensive use of this technique leads to essentially unambiguous indexing.

4.3. *Determination of triplet phases*

The objectives of our initial phase investigations (Nicolosi, 1982; Ladell, 1982; Post, 1982; Gong & Post, 1983) were limited to the separation of the 'observed' triplet phases into two groups. The phases of all triplets in either group were identical. Their nature ('positive' or 'negative') was not specified at the separation stage. Gradually, as more phases were determined, it became clear that, for r.l.p.s entering the Ewald sphere, positive phases were invariably associated with the 'attenuation followed by enhancement sequence'. These experimental findings are inconsistent with the theoretical predictions of Hummer & Billy (1982). The criteria outlined above were used to assign phases to the triplets listed in Table 1 and displayed in Fig. 4.

Peaks 1, 5, 8, 9 and 14 display relatively weak phase indications. Careful examination, however, reveals accumulations of intensity on one side of each of these maxima, near the background line. These characterize 'enhancement' for all maxima. In the cases cited, where the 'attenuation' is not displayed as clearly as might be desired, the phase assignments are based primarily on these intensity enhancements.

In previous investigations of the phases of germanium triplets by one of the authors (B. Post), only eight of the 17 phases were determined. The others were rendered indeterminate by the relatively high backgrounds and the effects of overlapping peaks in the n-beam patterns. Those patterns were recorded using polychromatic incident beams from 'fine-focus' sources, in conjunction with large source-to-detector distances. The latter reduced the incident-beam divergence to about 2′ and made possible the elimination of most $K\alpha_2$ from the diffracted beams.

The biaxial diffractometer provides an incident beam whose $K\alpha_2$ content we could not detect, and an incident-beam divergence of about 30 to 40″; these made possible the improved pattern shown in Fig. 4.

Efforts are under way to reduce the beam divergence to 10 and 15″. Under these conditions the angular range of primary radiation 'seen' by the detector should be of the order of the half-widths of most interactions. The sensitivity of apparatus to very weak interactions should then be greatly increased. It should also be noted that step sizes of 0·005° were used to record data shown in Fig. 4. These will be reduced, as needed, to 0·001° with corresponding improvements in resolution.

References

COLE, H., CHAMBERS, F. W. & DUNN, H. M. (1962). *Acta Cryst.* **15**, 138–144.

GONG, P. P. & POST, B. (1983). *Acta Cryst.* A**39**, 719–724.

HUMMER, K. & BILLY, H. W. (1982). *Acta Cryst.* A**38**, 841–848.

JAMES, R. W. (1963). *Solid State Phys.* **15**, 55–220.

LADELL, J. (1982). Am. Crystallogr. Assoc. Winter Meet. Abstract M8.

LADELL, J. (1984). In preparation.

NICOLOSI, J. A. (1982). Am. Crystallogr. Assoc. Winter Meet. Abstract M7.

POST, B. (1975). *J. Appl. Cryst.* **8**, 452–456.

POST, B. (1979). *Acta Cryst.* A**35**, 17–21.

POST, B. (1982). Am. Crystallogr. Assoc. Winter Meet. Abstract A1.

POST, B. (1983). *Acta Cryst.* A**39**, 711–718.

RENNINGER, M. (1937). *Z. Phys.* **106**, 141–176.

Acta Cryst. (1984). A**40**, 688-695

Enantiomorph-Dependent Probability Distributions of Origin-Invariant Phases

BY W. M. G. F. PONTENAGEL* AND H. KRABBENDAM

Laboratorium voor Structuurchemie, Rijksuniversiteit Utrecht, Padualaan 8, 3584 *CH Utrecht, The Netherlands*

AND J. J. L. HEINERMAN

Prinsenstraat 15^c, 1015 *DA Amsterdam, The Netherlands.*

(*Received* 28 *September* 1983; *accepted* 26 *June* 1984)

Abstract

By integrating joint probability distributions of two related invariant phases with respect to one of the variables over the range 0 to π, enantiomorph-dependent phase indications may be obtained. In the present paper the full potential of such a strategy is described. For probability distributions correct up to and including terms of order N^{-1}, all cases of interest appear to consist of combinations of two invariants with one or two structure factors in common. For each case the joint probability distribution of the phases of such a pair of invariants, given a number of suitable structure-factor amplitudes, is derived.

* Present address: DSM Research, Geleen, The Netherlands.

0108-7673/84/060688-08$01.50